

Origin of octahedral tilting in orthorhombic perovskites

B. Magyari-Köpe,¹ L. Vitos,^{2,3} B. Johansson,² and J. Kollár³

¹*Theory of Materials, Physics Department, Royal Institute of Technology, Stockholm Center for Physics, Astronomy and Biotechnology, SE-106 91, Stockholm, Sweden*

²*Applied Materials Physics, Department of Materials Science and Engineering, Royal Institute of Technology, SE-100 44 Stockholm, Sweden*

³*Research Institute for Solid State Physics and Optics, P.O. Box 49, H-1525 Budapest, Hungary*

(Received 16 May 2002; published 9 September 2002)

The adopted crystal structure of the ABO_3 perovskites is determined by the balance between the interaction of the semicore states of the A and B atoms and oxygen ions. Topological considerations show that the structural setup always stabilizes the cubic phase at large pressures, while small or negative pressures favor nonvanishing octahedral tiltings. As an example, we show that the structural distortion in $CaSiO_3$ perovskite is slightly depressed with hydrostatic pressure, but it increases significantly with increasing volume.

DOI: 10.1103/PhysRevB.66.092103

PACS number(s): 61.50.Ah, 71.15.Nc, 91.60.Ki

At ambient conditions relatively few of the ABO_3 systems adopt the ideal perovskite structure with $Pm\bar{3}m$ symmetry. A number of structural deviations presenting some kind of distortion have been observed. One of the most commonly observed perovskite structures has the orthorhombic $Pbnm$ symmetry. Within this space group, the octahedral tilting, originating from finite rotations of the BO_6 octahedra, is realized by preserving the central symmetry of the B cation, while the A cation “prefers” off-center displacements. In some perovskites the octahedral rotation can be very small, like in $CaSiO_3$,^{1–3} or vanish at relatively low pressure and temperature, like in $SrZrO_3$.⁴ In other perovskites the distortion is more significant and can develop with pressure or temperature to a less distorted, e.g., $ScAlO_3$ lattice,⁵ or to a more distorted, e.g., $MgSiO_3$,⁶ lattice.

The understanding of the mechanisms that lead to the stabilization of the various perovskite structures has been a long standing problem in material science. Due to the frequent occurrence of ABO_3 perovskites, and also to the great variety of properties presented by these systems, the accurate and transparent description of the driving forces toward the high or low symmetry crystal structures is of general interest. For instance, the pressure induced structural changes in mineral perovskites, e.g., $MgSiO_3$ and $CaSiO_3$, have important geophysical implications. These materials represent the primordial compositions in models for the dynamics and evolution of the Earth’s lower mantle, and for the observed discontinuities in this region.⁷

In order to describe the octahedral tilting in perovskite structures several phenomenological or semiempirical models have been developed.^{8–10} Recently, a very useful parametrization was introduced by Thomas.¹¹ Within the so-called *global parametrization method* (GPM) the lattice parameters are given as functions of the unit cell volume V and the polyhedral volume ratio. The latter is defined as the volume of the AO_{12} polyhedron, V_A , divided by the volume of the BO_6 octahedron, V_B . The polyhedral volume ratio is related to the individual tilt angles of the octahedron relative to the cubic axis $(\theta_x, \theta_y, \theta_z)$.¹² From V_A/V_B the degree of tilt is obtained as $\Theta \equiv 1 - \cos^2[(\theta_x + \theta_y)/2] \cos \theta_z$

$= (5 - V_A/V_B)/6$.^{3,11,13} For an undistorted lattice we have $V_A/V_B = 5$, while values below 5 correspond to finite octahedral tiltings. Recently, the GPM has been revised (revGPM) (Refs.12 and 14) and extended to describe the temperature and pressure dependence of the orthorhombic crystal structure of perovskites. The revGPM has been employed in conjunction with *ab initio* total energy methods^{15,16} in the description of the evolution of structural parameters with hydrostatic pressure. The remarkably good agreement between theoretical results^{3,5,12} and available experimental data for $MgSiO_3$ and $ScAlO_3$ perovskites, demonstrates the applicability of the revGPM scheme in the prediction of the crystal structure of orthorhombic and cubic perovskites.

In this paper the revGPM is combined with a simple model based on the *ionic overlaps* in order to analyze, at a qualitative level, the octahedral rotations in ABO_3 systems and to facilitate a deeper understanding of the origin of orthorhombic structural distortions at ambient conditions, and their variation with hydrostatic pressure.

We investigate the perovskite systems with cations from IIA-IVB, IIA-IVA, and IIIA-IIIB columns of the Periodic Table. Some of these perovskites are listed in Table I together with the size of orthorhombic distortion expressed as the V_A/V_B ratio. For example, at ambient conditions $MgSiO_3$ adopts the $Pbnm$ orthorhombic structure with $V_A/V_B \approx 4.3$. Experimentally, $CaSiO_3$ has been found to have the ideal cubic symmetry, and $CaGeO_3$ crystallizes in $Pbnm$ structure with $V_A/V_B \approx 4.7$. It follows from these data that the origin of distortions in perovskite systems should reside in the electronic structures of both A and B atoms, but also in a delicate balance between them. Since the bulk perovskites are mainly governed by ionic bonds, we concentrate on the electronic structure of the A and B ions, and demonstrate that these represent the key driving forces towards different perovskite structures.

We show that the structural distortions in perovskites can be accounted for by the relative overlap between the semicore states of A and B cations and the oxygen ions. We introduce the quantity

$$\omega_c(V, V_A/V_B) = r_c + r_O - d_{c-O}(V, V_A/V_B),$$

TABLE I. The equilibrium crystal structure of selected perovskite systems. The size of the octahedral tilting is expressed in terms of the polyhedral volume ratio V_A/V_B . η denotes the relative volume compression, where, according to the present model based on the ionic overlaps (see text), a possible orthorhombic-cubic phase transition occurs. [†]Small orthorhombic distortion.

IIa(A)	IVa,b(B)	Structure	V_A/V_B	Refs.	η (%)
Mg	Si	Orth.	4.28	21,11	64
Ca	Si	Cubic	5.00 [†]	22,1	-
Ca	Ge	Orth.	4.71	4	14
Sr	Ge	Cubic	5.00 [†]	23	-
Sr	Sn	Cubic	5.00 [†]	24–26	12
Ba	Sn	Cubic	5.00	26	-
Sr	Zr	Orth.	4.82	4	25
Ba	Zr	Cubic	5.00	4	-
Ca	Ti	Orth.	4.61	11	42
Sr	Ti	Cubic	5.00	4,27	-

IIIa(A)	IIIb(B)	Structure	V_A/V_B	Ref.	η (%)
Sc	Al	Orth.	4.08	28	83
Y	Al	Orth.	4.47	11	52

where c stands for A or B . r_A , r_B , and r_O denote the effective ionic radii, and d_{A-O} and d_{B-O} are the cations and nearest-neighbors oxygen bond lengths. These distances depend on the volume of the unit cell and on the crystal symmetry. The V_A/V_B dependence of d_{A-O} and d_{B-O} , calculated within the revGPM, is shown in Fig. 1.

Zero pressure. First we discuss the symmetry dependence of ω_A and ω_B at constant (zero) pressure. Consider an ABO_3 perovskite in the ideal crystal structure with $V_A/V_B \approx 5$ having $\Delta\omega \equiv \omega_B - \omega_A > 0$. In this system the B cation is compressed relative to the A cation, which gives rise to a repulsive interaction between the B ion and the neighboring oxygens. The existence of the repulsive cation-oxygen inter-

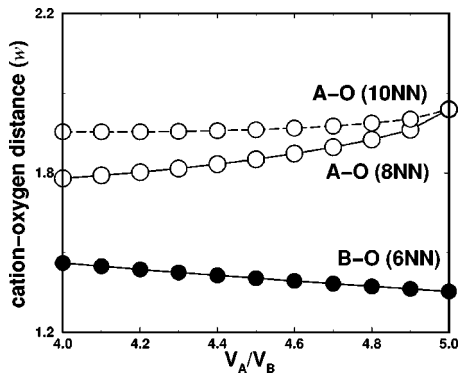


FIG. 1. The V_A/V_B dependence of the average cation-oxygen distances d_{A-O} (open circles) and d_{B-O} (filled circles). The d_{A-O} distances have been determined for the first eight (8NN) and for the first ten (10NN) nearest-neighbor oxygens as well. The distances have been calculated at constant volume and expressed in units of the average Wigner-Seitz radius w . For cubic perovskites (i.e., for $V_A/V_B = 5.0$) $d_{A-O} = \sqrt{2}a/2$ and $d_{B-O} = a/2$, where $a = (20\pi/3)^{1/3}w$ is the cubic lattice parameter.

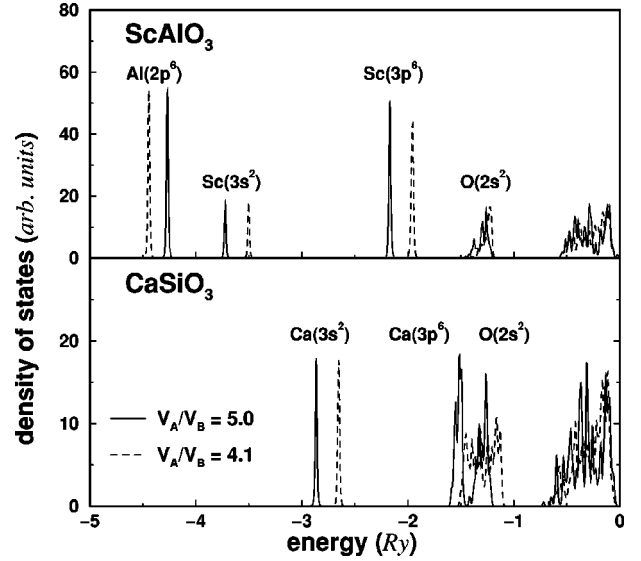


FIG. 2. The density of states of $ScAlO_3$ and $CaSiO_3$ calculated at the experimental equilibrium volume for $V_A/V_B = 5.0$ (solid lines) and $V_A/V_B = 4.1$ (dashed lines). The $2p^6$, $3s^2$, and $3p^6$ semicore states of cations and the $2s^2$ band of oxygen are marked.

action has already been pointed out by earlier studies.^{9,17} For illustration, in Fig. 2 we plotted the zero pressure density of states¹⁸ of $ScAlO_3$ for two different V_A/V_B ratios (upper panel). It follows that when V_A/V_B increases from 4.1 to 5.0 the $2p^6$ semicore states of Al approach the valence states, which results in an increase in the kinetic energy.

Now the ABO_3 system can reduce the large $\Delta\omega$ and equilibrate the microscopic stresses around the B cation by lowering $d_{A-O} - d_{B-O}$. In accordance with Fig. 1, at constant volume this can be realized by lowering the V_A/V_B ratio, i.e. by a finite tilting of the BO_6 octahedra relative to the cubic axis. The size of the deformation, on the other hand, is determined by the electronic structure of the A cation. That is, by lowering $\Delta\omega$ the overlap of the A cation becomes more pronounced compared to that of the B cation, and this shifts the semicore states of A toward the valence states. This effect is shown in Fig. 2 in the case of $ScAlO_3$ (upper panel) and $CaSiO_3$ (lower panel). The energetically unfavorable offsets of the $3s^2$ and $3p^6$ states of Sc and Ca with decreasing V_A/V_B oppose the symmetry lowering tendencies of the $2p^6$ semicore states of Al and Si (not shown for Si).

Therefore, the ABO_3 system reaches its thermodynamic equilibrium as a balance of the repulsive interactions between the cations and the surrounding oxygens. At a constant volume this can be realized by optimizing the overlaps between the A and B cations with the neighboring oxygen ions. Consequently, according to the present model, zero or negative $\Delta\omega$'s (calculated for $V_A/V_B \approx 5$) lead to cubic or barely distorted perovskites, while positive $\Delta\omega$ induces a symmetry lowering deformation.

In order to demonstrate the correlation between $\Delta\omega$ and the adopted crystal structure, in Fig. 3 we have plotted the experimentally observed low pressure V_A/V_B ratios for a series of cubic and orthorhombic perovskites as functions of $\Delta\omega$. In each case the linear overlap was evaluated for the

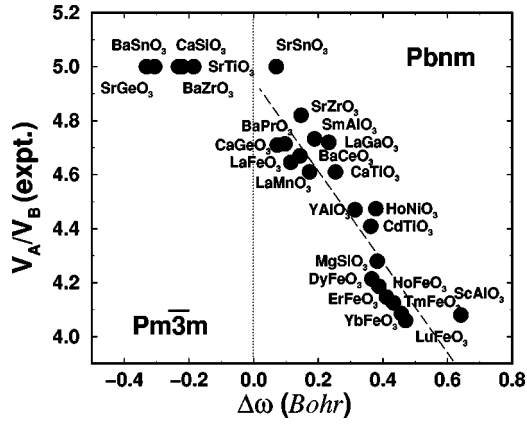


FIG. 3. The correlation between the relative linear overlap $\Delta\omega$ (in units of Bohr) and the experimental polyhedral volume ratio V_A/V_B . $\Delta\omega$ is calculated for a cubic structure with a volume equal to the experimental equilibrium volume. The dashed line, corresponding approximately to $5.0 - 1.7\Delta\omega/B$, is a linear fit to the non-cubic perovskites.

$Pm\bar{3}m$ structure at the experimental equilibrium volume, and for the ionic radii we used the data from Ref. 19. It follows from the figure that negative values of $\Delta\omega$ correspond to cubic ($BaSnO_3$, $BaZrO_3$, and $SrTiO_3$) or nearly cubic ($SrGeO_3$ and $CaSiO_3$) perovskites, while positive $\Delta\omega$ indicate some extent of orthorhombic lattice distortion. In fact we find that the $\Delta\omega$ versus experimental V_A/V_B plot is nearly linear for $\Delta\omega > 0$. These results are in perfect accordance with the present model.

Positive pressures. Next we consider the volume/pressure dependence of ω_A and ω_B . In a cubic lattice, $d_{A-O} = \sqrt{2}d_{B-O}$, and, accordingly, ω_A increases faster than ω_B with hydrostatic pressure. Hence, the originally large $\Delta\omega$, corresponding to a distorted perovskite structure, always decreases with decreasing volume. According to Fig. 3 a lower $\Delta\omega$ indicates a smaller octahedral tilt. Thus the present model predicts that the hydrostatic pressure drives the system towards a less distorted crystal structure in any ABO_3 type of perovskite.

The distortion reducing effect of the hydrostatic pressure has been reported in several experimental studies. For instance, in $CaGeO_3$, $SrZrO_3$, $CaTiO_3$ and $YAlO_3$, the octahedral rotation decreases with pressure.^{4,11} However, there are a few cases, like $MgSiO_3$, where in the stability region (for pressures above 23 GPa) the structural distortion slightly increases with compression.¹² We ascribe this anomalous behavior to the more localized nature of the semicore states in Mg compared to the semicore states in Ca, Sr, Ba, Sc, Y, etc. The hardening of the MgO_{12} polyhedron relative to the SiO_6 octahedra would occur only at extremely high pressures.

Within the present model, for any perovskite system one can determine the critical volume V_c , where $\Delta\omega$ vanishes. As the ABO_3 system approaches this volume, the balance of the cation-oxygen interactions occurs already at large polyhedral volume ratio, i.e. at $V_A/V_B \approx 5$. Therefore, in the vicinity of this volume the octahedral tilt gradually disappears, and an orthorhombic-cubic phase transition may take place. We note that the present model does not exclude the appear-

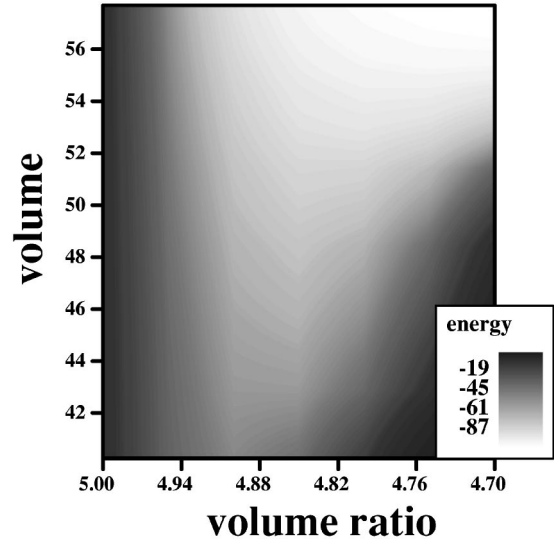


FIG. 4. The total energy (in meV per formula unit) of orthorhombic $CaSiO_3$ perovskite as a function of volume (in \AA^3) and polyhedral volume ratio V_A/V_B (dimensionless). At each volume the energies are given relative to the energy of the cubic phase ($V_A/V_B = 5.0$).

ance of intermediate phases with, e.g., tetragonal, rhombohedral, or hexagonal symmetry. The critical volume can be estimated from the condition $\Delta\omega(V_c, 5) \approx 0$, i.e., $r_B - r_A + [(\sqrt{2} - 1)/2]V_c^{1/3} \approx 0$. The volume compressions $\eta = (V_0 - V_c)/V_0$, corresponding to possible phase transitions, are listed in the last column of Table I. According to these data the orthorhombic $SrZrO_3$, for example, transforms to the cubic phase at about $\eta = 25\%$, compared to the experimental value of 19-23%.⁴ We predict that $CaGeO_3$ and $SrSnO_3$ also transform to a cubic structure at relatively low pressures. However, the rest of the orthorhombic perovskites from Table I will remain distorted up to high pressures and in some cases ($MgSiO_3$ and $ScAlO_3$) extremely high pressures.

Negative pressures. We have shown that orthorhombic perovskites tend to transform to a less distorted structure and finally to the high symmetry cubic structure at high pressures. Nevertheless, as volume is increased, *viz.* at negative pressures, all perovskites tend to adopt a more distorted structure. This universal behavior emerges directly from the present model based on relative *ionic overlaps*. Since $\Delta\omega$ increases linearly with $V^{1/3}$, negative pressures produce large stresses around the B cation from the cubic lattice, which are reduced by further structural distortions.

We demonstrate the distortion enhancing effect of negative pressures in the case of $CaSiO_3$ perovskite. The predicted ground state structure of $CaSiO_3$ is of cubic symmetry (see Fig. 3) in agreement with experimental results.²⁰ However, the most recent *ab initio* calculations^{1,3} indicate the presence of small lattice distortions with $V_A/V_B \approx 4.9$. It has been shown that the average tilting of the SiO_6 octahedra relative to the cubic axis is gradually reduced with pressure.³ Here we investigate the effect of negative pressures on the crystal structure of $CaSiO_3$ using the revGPM in conjunction with the *exact muffin-tin orbital* total energy method.^{15,16} In

Fig. 4 we show the total energies of CaSiO_3 relative to the total energies of the cubic phase as a function of the unit cell volume and the polyhedral volume ratio. The theoretical equilibrium volume of CaSiO_3 is $V_0 = 45.85 \text{ \AA}^3$, and the volume range in Fig. 4 corresponds approximately to pressures between -25 and 40 GPa. The hydrostatic pressures have been estimated from the cubic equation of states from Ref. 3. At polyhedral volume ratios between approximately 4.9 and 4.7 the volume dependent minima of the total energy mark the volume dependence of the equilibrium octahedral rotations relative to the ideal cubic structure. At positive pressures, i.e., $V > V_0$, the lattice distortion decreases slightly with pressure, but the octahedral tilt is still not totally suppressed at the smallest volume considered. However, when the volume is increased beyond the equilibrium value, the crystal structure deviates more and more from the high symmetry cubic phase. For $(V_0 - V)/V_0 = -26\%$, i.e., a pressure about -25 GPa, the polyhedral ratio falls below 4.7.

Conclusions. We have presented a model of the origin of octahedral rotation in orthorhombic perovskite structures. The model is based on the relative *ionic overlaps* and the *global parametrization method*, and is supported by *ab initio* total energy calculations. It gives a very good estimate of the

amount of distortion exhibited by perovskite systems at ambient pressure. Furthermore, it reproduces well the pressure dependence of the lattice distortions, and describes structural phase transitions in close agreement with the experimental observations. We predict that (a) hydrostatic pressure always stabilizes the less distorted structures, and (b) negative pressure favors large octahedral rotations. This universal bond picture of perovskites is a simple consequence of the balance of the interactions between the semicore states of the cations and oxygen ions. In real perovskites, however, the size of these interactions can be modulated by the nature of the semicore states (*s*, *p*, *d*, or *f* orbitals) and also by the non-ionic character of the cation-oxygen bonds (e.g., the presence of *d* orbitals).

The Swedish Natural Science Research Council, the Swedish Foundation for Strategic Research, and the Royal Swedish Academy of Sciences are acknowledged for financial support. Part of this work was supported by the research project OTKA T035043 of the Hungarian Scientific Research Fund, the Hungarian Academy of Science, and the EC Centre of Excellence program (No. ICA1-CT-2000-70029). The calculations were performed at the Swedish National Supercomputer Center, Linköping, and the Hungarian National Supercomputer Center, Budapest.

-
- ¹L. Stixrude *et al.*, Am. Mineral. **81**, 1293 (1996).
 - ²A.V.G. Chizmeshya *et al.*, Geophys. Res. Lett. **23**, 2725 (1996).
 - ³B. Magyari-Köpe *et al.*, Phys. Rev. B **65**, 193107 (2002).
 - ⁴D. Andrault and J.P. Poirier, Phys. Chem. Miner. **18**, 91 (1991).
 - ⁵B. Magyari-Köpe, L. Vitos, B. Johansson, and J. Kollár, J. Geophys. Res. **107**(B7), 10.1029/2001JB000686 (2002).
 - ⁶L. Stixrude and R.E. Cohen, Nature (London) **364**, 613 (1993).
 - ⁷E. Knittle *et al.*, Nature (London) **319**, 214 (1986).
 - ⁸A.M. Glazer, Acta Crystallogr., Sect. B: Struct. Crystallogr. Cryst. Chem. **28**, 3384 (1972); **31**, 756 (1975).
 - ⁹P.M. Woodward, Acta Crystallogr., Sect. B: Struct. Sci. **53**, 44 (1997).
 - ¹⁰C.J. Howard and H.T. Stokes, Acta Crystallogr., Sect. B: Struct. Sci. **54**, 782 (1998).
 - ¹¹N.W. Thomas, Acta Crystallogr., Sect. B: Struct. Sci. **52**, 16 (1996); **54**, 585 (1998).
 - ¹²B. Magyari-Köpe *et al.*, Acta Crystallogr., Sect. B: Struct. Sci. **57**, 491 (2001).
 - ¹³B. Magyari-Köpe *et al.*, in *Perovskite Materials*, edited by K. Poeppelmeier, A. Navrotsky, and R. Wentzcovitch, MRS Symposia Proceedings No. 718 (Materials Research Society, Pittsburgh, 2002).
 - ¹⁴B. Magyari-Köpe, L. Vitos, B. Johansson, and J. Kollár, Comput. Mater. Sci. (to be published).
 - ¹⁵L. Vitos, Phys. Rev. B **64**, 014107 (2001).
 - ¹⁶O. K. Andersen *et al.*, G. Krier, in *Lectures on Methods of Electronic Structure Calculations*, edited by V. Kumar, O. K. Andersen, A. Mookerjee (World Scientific, Singapore, 1994), p. 63.
 - ¹⁷M.W. Lufaso and P.M. Woodward, Acta Crystallogr., Sect. B: Struct. Sci. **57**, 725 (2001).
 - ¹⁸The self-consistent density of states of ScAlO_3 and CaSiO_3 were calculated using the *exact muffin-tin orbital* electronic structure method (Ref. 15 and 16) within the local density approximation for the exchange-correlation term.
 - ¹⁹R.D. Shannon, Acta Crystallogr., Sect. B: Struct. Crystallogr. Cryst. Chem. **32**, 751 (1976).
 - ²⁰Y. Wang *et al.*, J. Geophys. Res. **101**, 661 (1996).
 - ²¹Y. Kudoh *et al.*, Phys. Chem. Miner. **14**, 350 (1987).
 - ²²S.-H. Shim, T.S. Duffy, and G. Shen, J. Geophys. Res. **105**, 25 955 (2000).
 - ²³A. Grzechnik *et al.*, J. Phys.: Condens. Matter **10**, 221 (1998).
 - ²⁴M. Leoni *et al.*, J. Mater. Sci. Lett. **15**, 1302 (1996).
 - ²⁵A. Vagas *et al.*, Acta Crystallogr., Sect. B: Struct. Sci. **42**, 511 (1986).
 - ²⁶C.P. Udawatte *et al.*, Solid State Ionics **128**, 217 (2000).
 - ²⁷D. de Ligny and P. Richet, Phys. Rev. B **53**, 3013 (1996).
 - ²⁸B. Magyari-Köpe *et al.*, Phys. Rev. B **63**, 104111 (2001).